

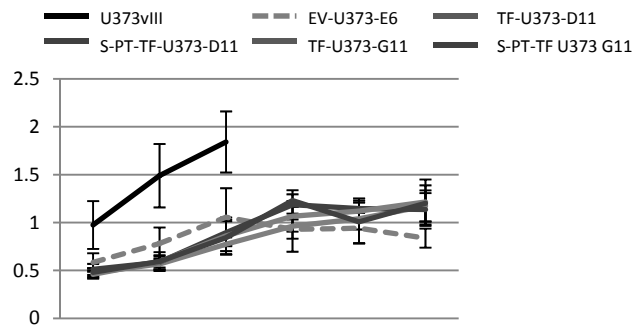
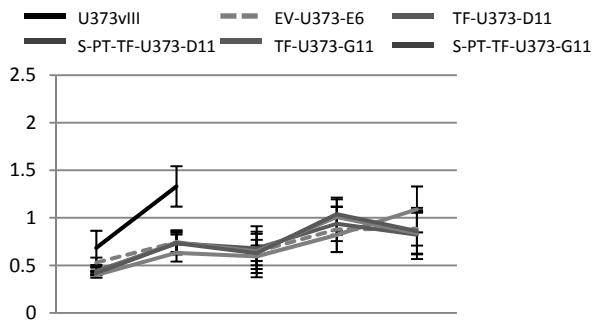
## **SUPPLEMENTARY FIGURES AND TABLES**

**Table S1: Characteristics of dormant, latent and aggressive glioma cell populations**

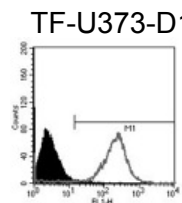
<b>Cell Line</b>	<b>Derivation</b>	<b>TF Level (FACS Mean Channel)</b>	<b>TF PCA (% pos. ctrl)</b>	<b>Mice Tested (N)</b>	<b>Tumor Take (%)</b>	<b>Tumor Detection (day)</b>
<b>U373</b>	Negative Control	17	15-30	5	0/5 (0%)	none
<b>EV-U373</b>	Transfection Control	12	15-30	9	1/9 (11%)	145
<b>TF-U373-D8</b>	Low TF Transfected Clone	24	15-30	5	0/5 (0%)	none
<b>TF-U373-F7</b>	Low TF Transfected Clone	NA	15-30	5	0/5 (0%)	none
<b>U373vIII</b>	Positive Control	94	100	12	12/12 (100%)	22-30
<b>TF-U373-F9</b>	High TF Transfected Clone	NA	80-100	5	3/5 (60%)	150-210
<b>TF-U373-D11</b>	High TF Transfected Clone	206	80-100	13	11/13 (85%)	120-191
<b>TF-U373-G11</b>	High TF Transfected Clone	253	80-100	14	13/14 (93%)	68-84
<b>TF-U373-G2</b>	High TF Transfected Clone	82	80-100	4	3/4 (75%)	90-120
<b>TF-U373-B2</b>	High TF Transfected Clone	277	90-100	4	4/4 (100%)	60-90
<b>S-PT-TF-U373-D11</b>	Primary Tumor Cell Line	377	50-90	5	5/5 (100%)	30-64
<b>S-PT-TF-U373-G11</b>	Primary Tumor Cell Line	225	50-90	10	10/10 (100%)	23-39

**A 10%FBS –Normoxia 5% O2**

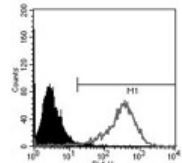
**B 10%FBS –Hypoxia 0.3%**



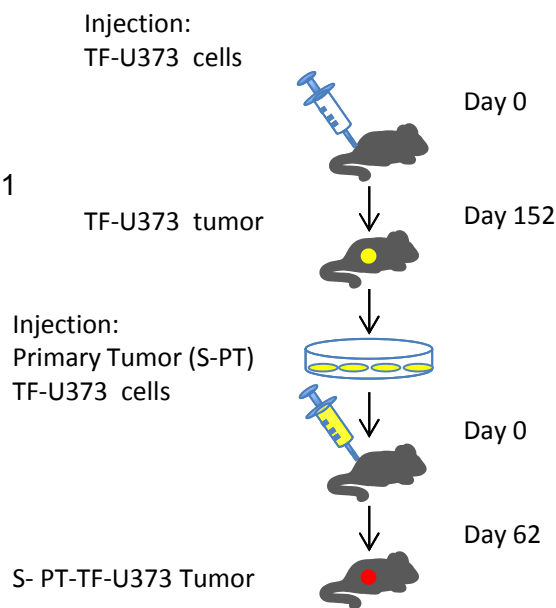
**C TF-U373-D11**



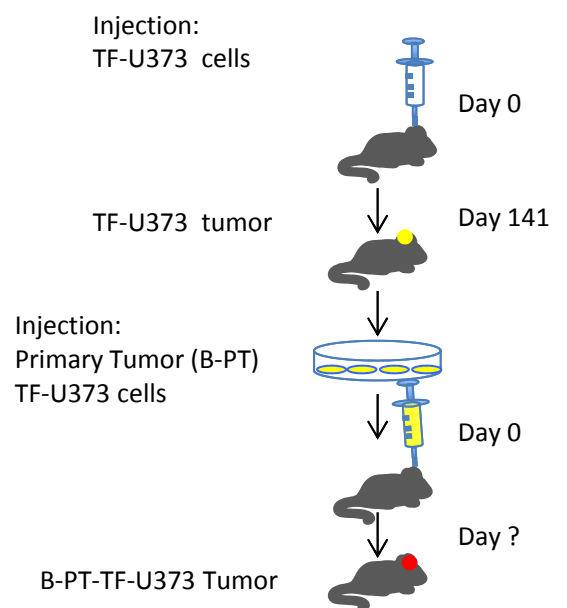
**S-PT-TF-U373-D11**



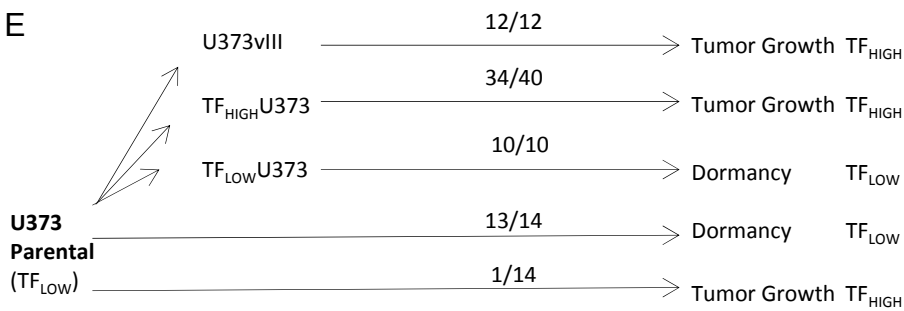
**D Subcutaneous-PT (S-PT) TF U373 Generation**



**Brain-PT (B-PT) TF-U373 Generation**



**E**



**F**

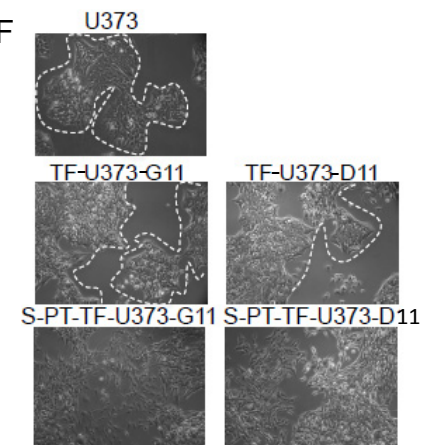
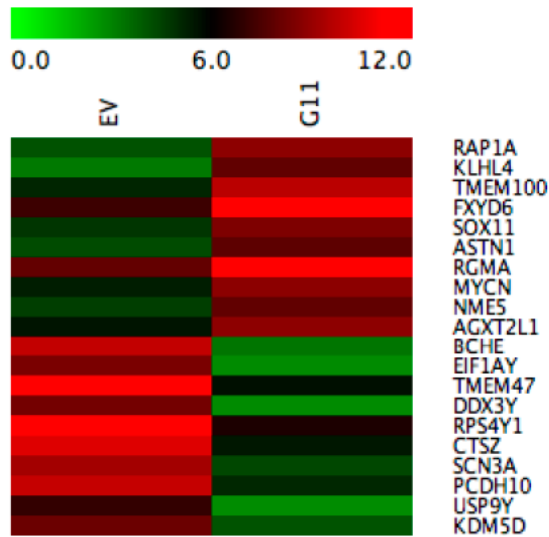


**Figure S1**

A



B

## Validated Genes

Molecules	FC
KLHL4*	24.954
SOX11*	13.107
MYCN*	10.977
NME5	9.91
AGXT2L1	9.447
RPS4Y1	-41.932
SCN3A*	-28.956

C

Network #	Network Type	Score
1	Cellular Movement, Genetic Disorder, Neurological Disease	87
2	Cell Movement, Cancer, Immune Cell Trafficking	56
3	Cancer, Cellular Growth & Proliferation, Cellular Development	53

Figure S2

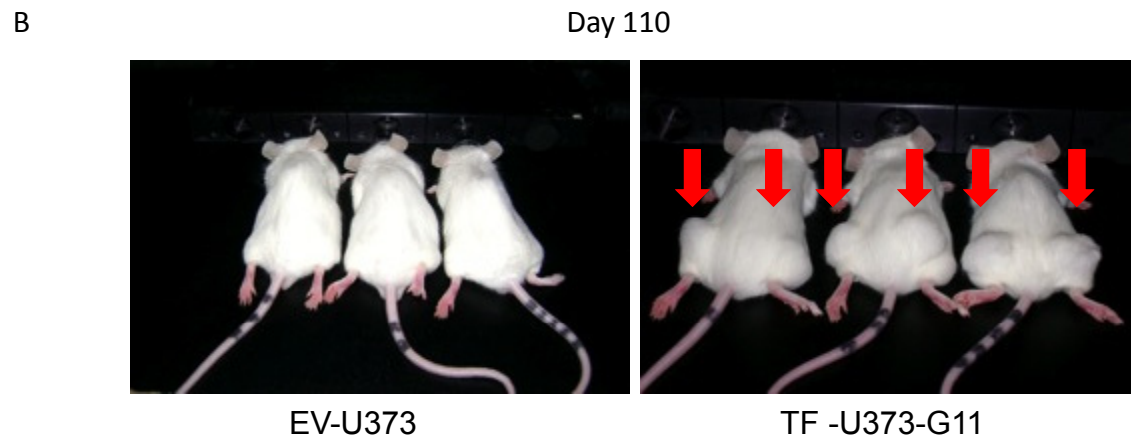
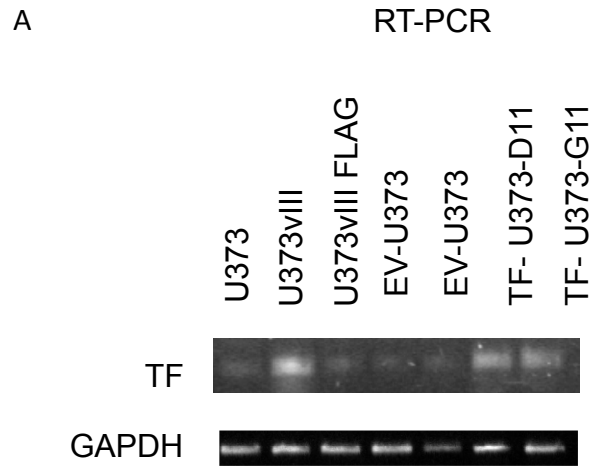


Figure S3

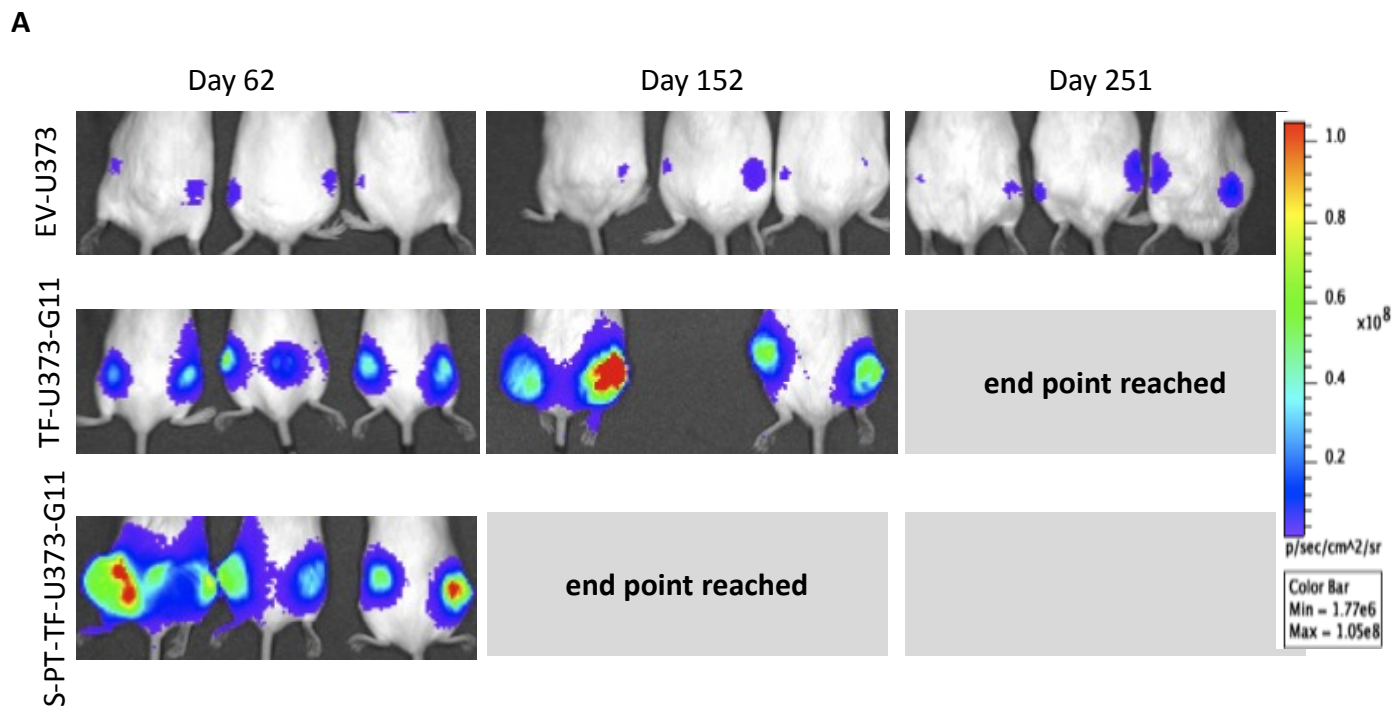


Figure S4

Day 16: EV-U373 to TF-U373-G11

**NETWORK 1: Cellular Movement, Genetic Disorder, Neurological Disease**

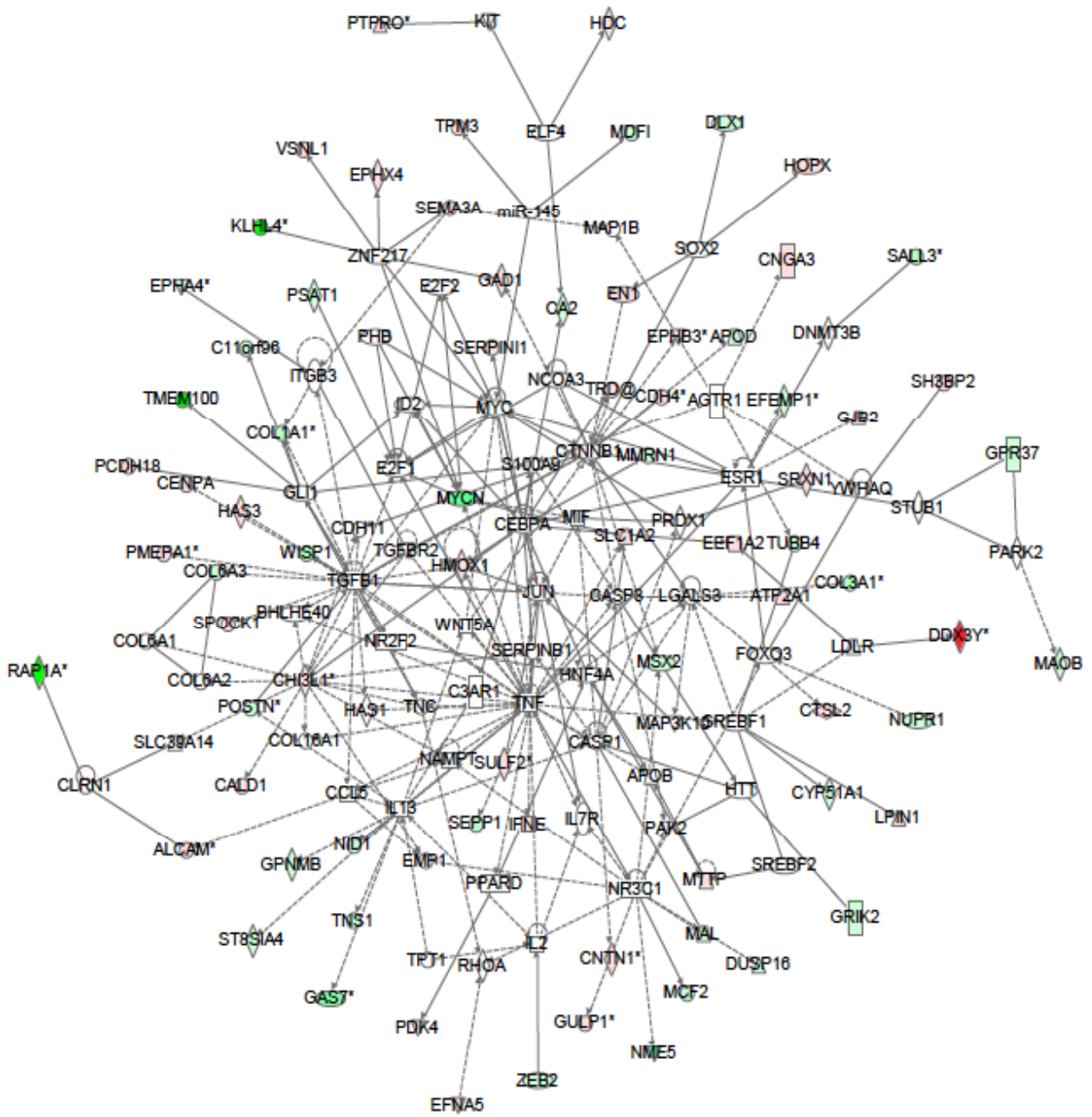


Figure S5

Day 16: EV-U373 to TF-U373-G11

**NETWORK 2: Cell Movement, Cancer, Immune Cell Trafficking**

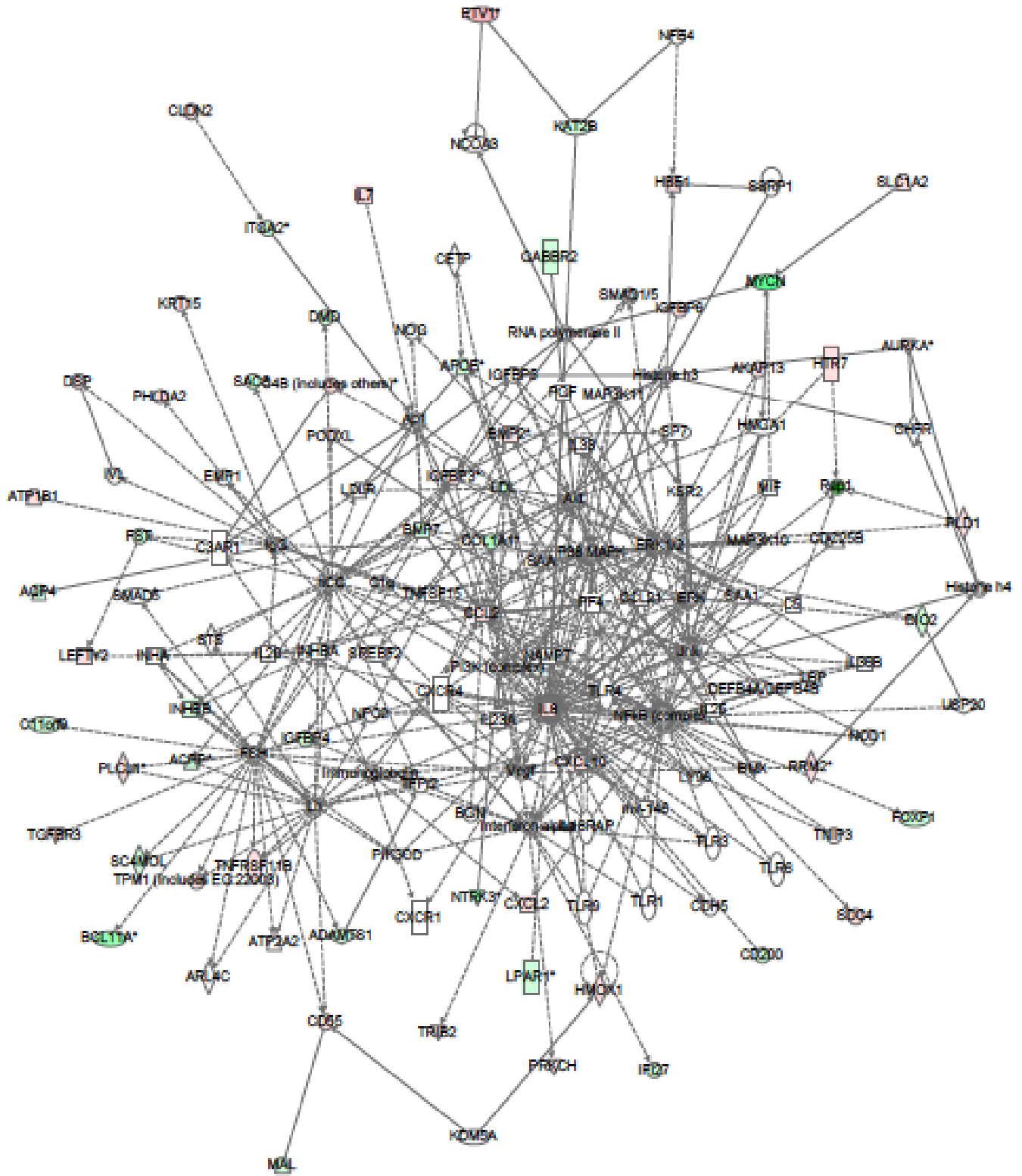


Figure S6



Day 16: EV-U373 to TF-U373-G11

### NETWORK 3: Cancer, Cellular Growth & Proliferation, Cellular Development

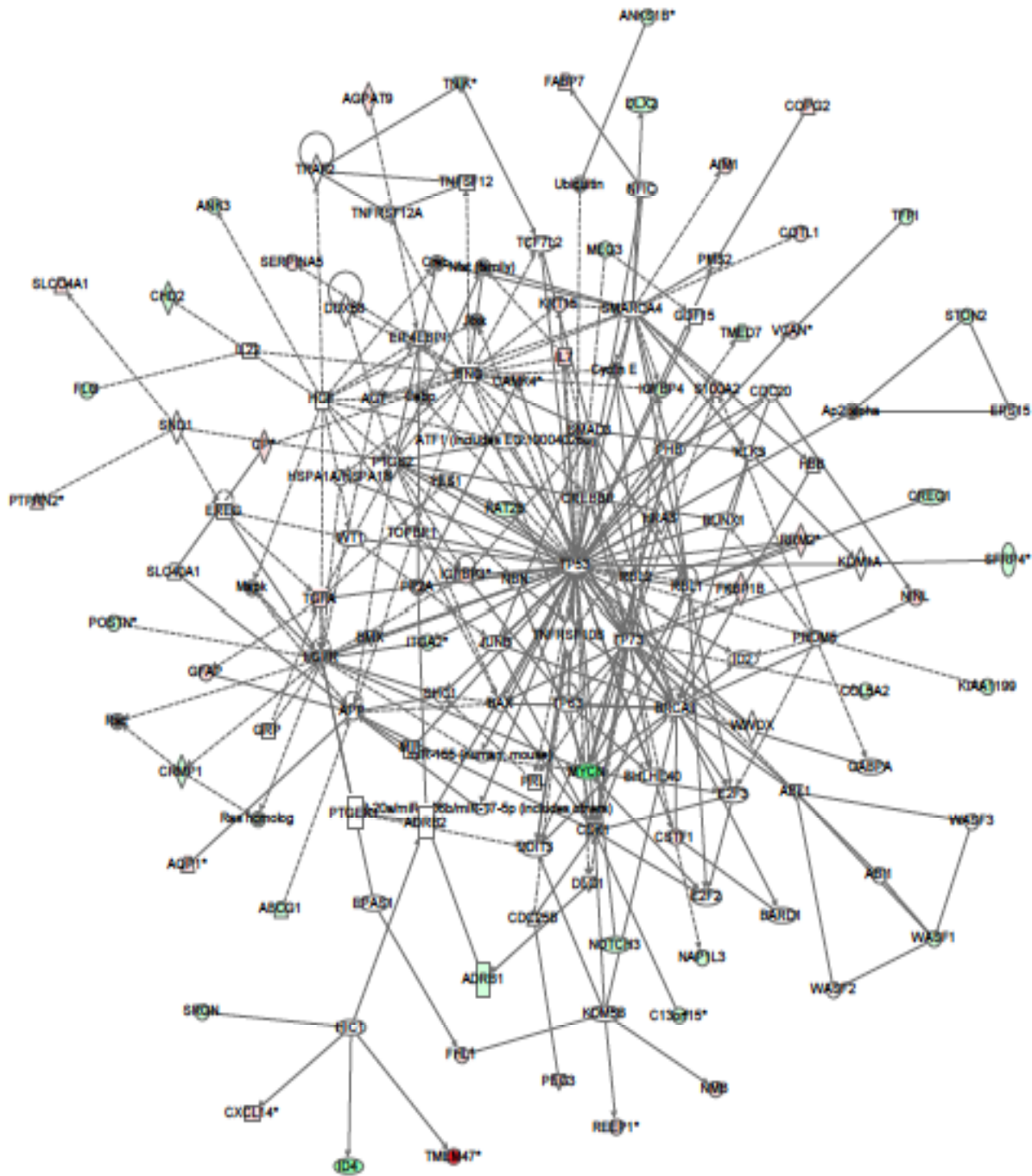


Figure S7

Day 16: TF-U373-G11 to S-PT-TF-U373-G11  
NETWORK 1: Cancer, Gene Expression, Cell Cycle

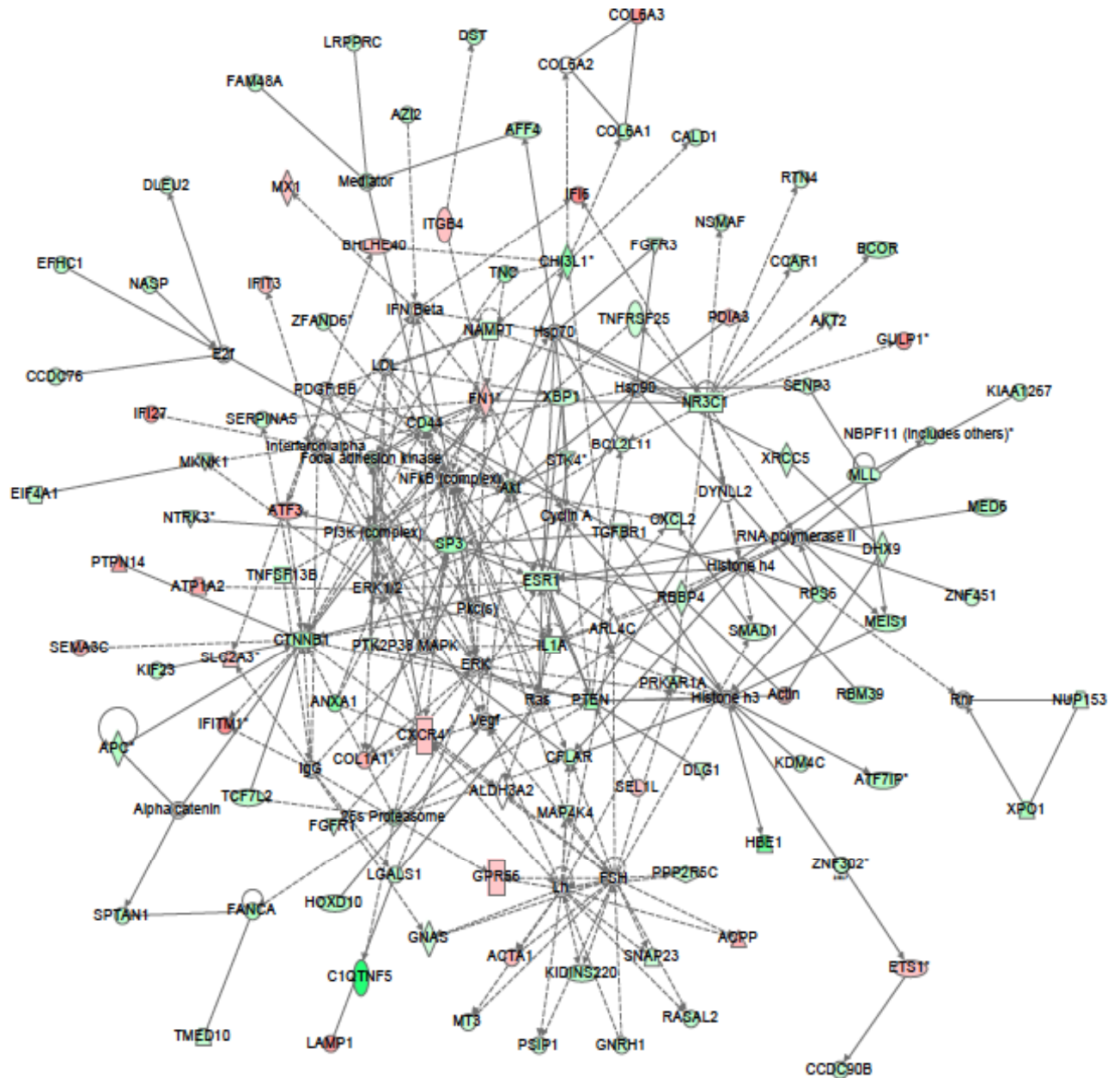


Figure S8

Day 16: TF-U373-G11 to S-PT-TF-U373-G11

**NETWORK 2: Inflammatory Response, Cellular Movement, Cancer**

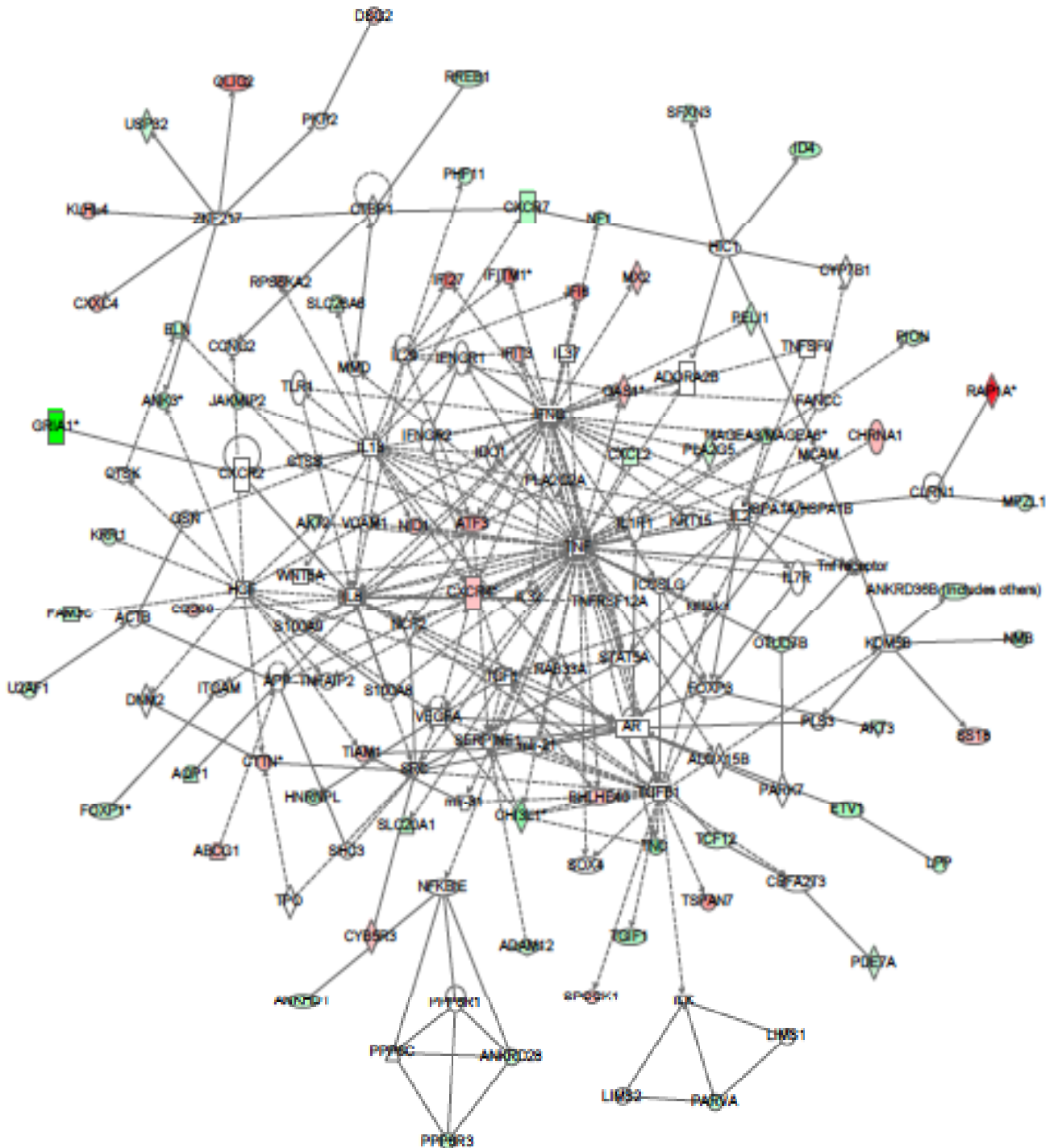


Figure S9

Day 16: TF-U373-G11 to S-PT-TF-U373-G11  
NETWORK 3: Cell Cycle, Cell Death, Cellular Growth & Proliferation

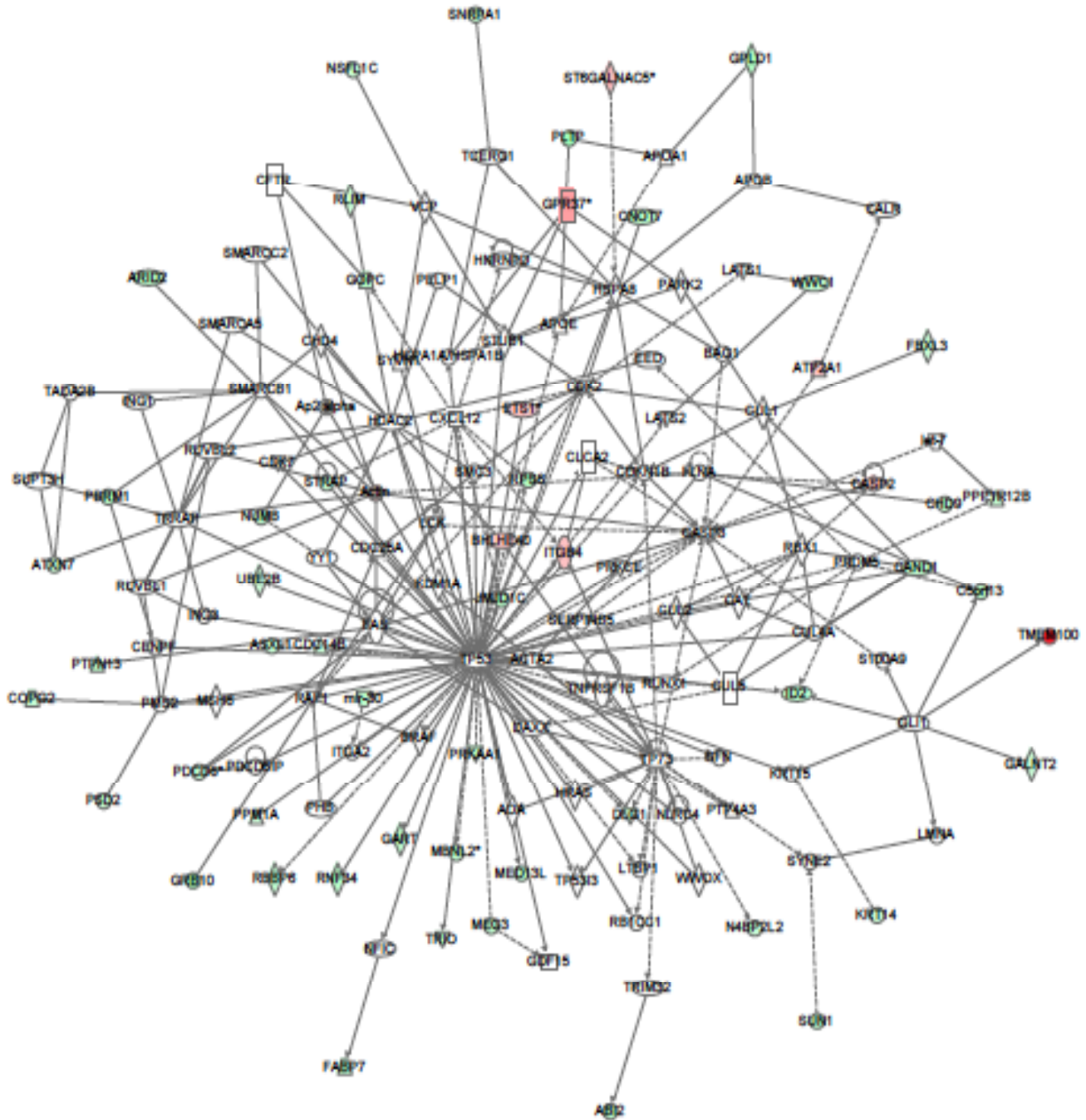
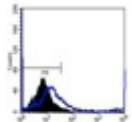
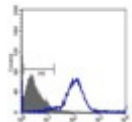
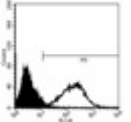
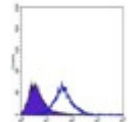
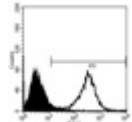
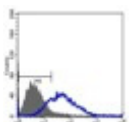
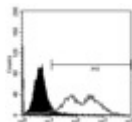
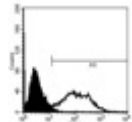
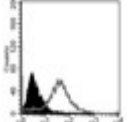
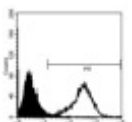
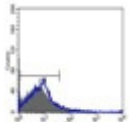
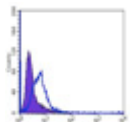
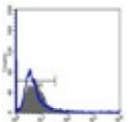
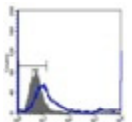
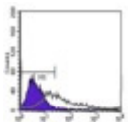
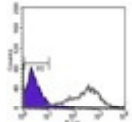


Figure S10

Table S2: Dormancy and TF expression in different cell models

	DORMANT	LATENT		PROGRESSIVE
GLIOBLASTOMA	 EV-U373	 TF-U373-G11	 TF-U373-B2	 S-PT-EV-U373
		 TF-U373-D11	 T98G	 S-PT-TF-U373-G11
		 TF-U373-G2	 SF188	 S-PT-TF-U373-D11
MELANOMA	 WM35			 WM35P3N2
	 WM1431B			 WM1431P3N2
COLORECTAL CARCINOMA	 HkH2 neg			 HkH2 pos
	TF NEGATIVE/LOW	TF POSITIVE/HIGH		

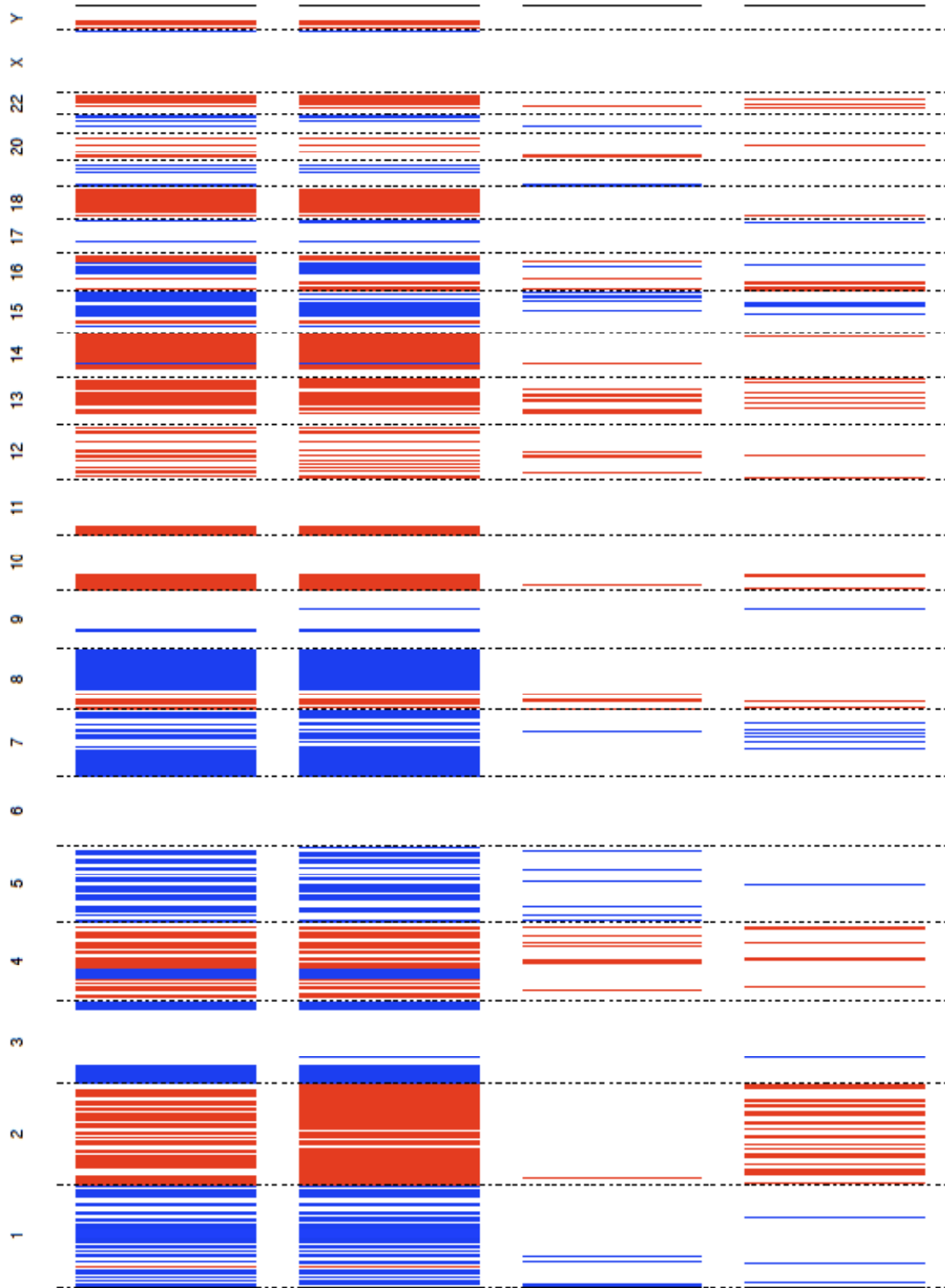


Figure S11

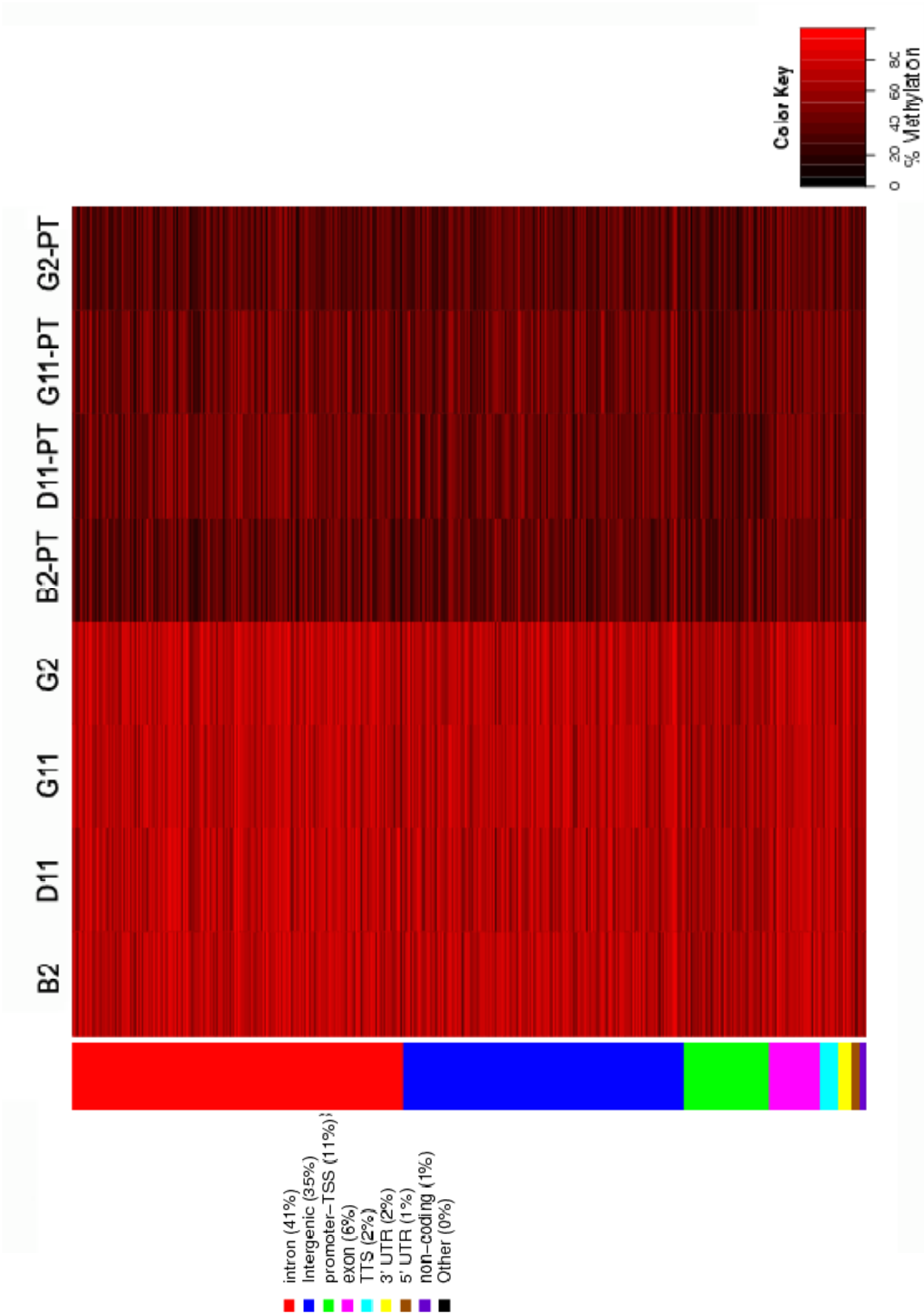
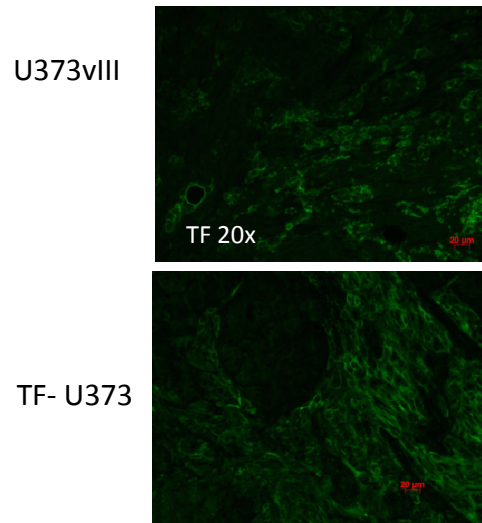


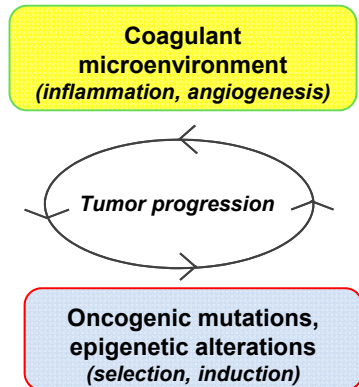
Figure S12



**Diversity of TF levels in vivo among glioma cells expressing uniform levels of TF in vitro** – U373vIII cells express uniform and high level of TF in culture. However, while growing as tumors in mice some of the cells remain brightly positive for TF antigen while the signal for other cells is somewhat diminished. Similar properties were observed in other TF-expressing glioma cells (compare Table S1) and were described in our earlier study (Milsom et al *Cancer Res.* 2008).

Figure S13





**Reciprocal interrelationship between microenvironment and cancer cell genome – a hypothesis.** TF-driven procoagulant microenvironment triggers inflammatory, angiogenic and other extracellular pressures that induce and select for genetic and epigenetic changes within cancer cells. This genotypic drift affects coagulant, inflammatory and angiogenic aspects of the cellular phenotype and secretome, which may further alter tumor microenvironment leading to adaptive cycles of tumor progression (vicious circle).

Figure S14

## **SUPPLEMENTAL MATERIALS AND METHODS:**

***Cell Lines and Cell Culture Conditions:*** All cell lines were maintained under standard culture conditions unless otherwise indicated. Cells were passaged at 70-80% confluency, usually on a biweekly basis, and to not exceed 30 consecutive subculturing. When necessary, cell cultures were trypsinized using 0.05% trypsin-EDTA solution (GIBCO), for 10 minutes at 37°C, DMEM media (10% FBS) was then added to counteract the effect of trypsin-EDTA. Cells were then spun at 1000rpm for 10 minutes in a refrigerated centrifuge (Sorvall RT 6000D, Dupont), re-suspended in growth medium and re-plated in T-75 flask at a 1:10 dilution. U373vIII cell lines were maintained in DMEM media (10% TET-free FBS; Multicell) along with antibiotics (Penicillin-Streptomycin 5%, GIBCO), geneticin/G418 (5ug/ul, GIBCO) and hygromycin (5ug/ul, Invitrogen). TF-U373 and Empty Vector cell lines were maintained with DMEM media (10% FBS) along with antibiotics, including hygromycin (10ug/ul, Invitrogen) as above.

T98G, U373, U87, SF-188, U343, U118, HkH2 and NHA cells were maintained in DMEM media with 10% FBS (MULTICELL) and 1% Pen Strep solution (GIBCO). WM35, WM351431B, WM35P3N2 cells were maintained in RPMI media with 5% FBS and 1% Pen Strep. Hypoxia treatment was conducted on cells plated on 96 well plate at 2,000 cells per well and grown at 1%O<sub>2</sub>, 37C and MTS assay conducted on days: 0, 2, 4, 6 and 8.

***FACS Analysis:*** Cells were grown to 70% confluency they were washed twice with PBS (pH 7.4), trypsinized and counted. Samples were aliquoted, so that 1.4x10<sup>6</sup> cells per sample were analysed. The samples were spun at 1000 rpm for 5 minutes to remove the media, which was replaced by a 1mL of PBS+1%BSA+0.1% azide, vortexed and re-spun twice in order to remove the residual media. Cell samples were mixed and incubated for 40 min on ice with 100uL of 1:200 of mouse anti-human TF antibody (American Diagnostica 4509 Mouse Anti-Human). Controls included unstained cells and cells

incubated with only the secondary antibody for each cell line used. Cells were spun, mixed and washed with PBS+1%BSA+0.1% three times before 100uL of 1:200 secondary antibody (Goat Anti-Mouse Alexa Fluor 488nm) was added to cell pellets for 30 minutes in a dark ice container. Washing in PBS+1%BSA+0.1% and another wash with a serum-free PBS+0.1% azide solution followed this. A 1mL solution of PBS+0.1% azide and 1% PFA fixative was then added to the cells for 30 minutes, at 37°C. Samples were then washed one more time and passed through a 30 um mesh into 5mL FACS tubes to remove aggregates. Samples were analyzed using a FACS Calibur Flow Cytometer (Becton Dickinson).

**MTS Assay:** The rate of proliferation of cell lines was measured following normoxic, hypoxic and starvation growth conditions using a CellTiter 96® Aqueous Non-Radioactive Cell Proliferation Assay (MTS) (PROMEGA). The principle of this assay rests on generation of formazan from MTS (which is added to cells prior to readings). The conversion of MTS into the aqueous soluble formazan product is catalysed by dehydrogenase found in metabolically active cells, the amount of which reflects the number of living cells in culture. One thousand cells per well was plated in five 96 well dishes and incubated overnight at 37°C. Each day a plate was taken and read at 492nm using a Lab systems Multiskan BIOCHROMTIC 1.03 plate reader.

**Transfections:** . (i) *Tissue factor:* Stable transfections were carried out using pcDNA3.1/Hygro vector containing full-length human tissue factor. An empty vector was used for control (mock) transfections. Cells were grown on 6 well (FALCON) plates to 70% confluency, at which point they were starved with 0% FBS media overnight. The cultures were exposed to 1 ug/ul of pcDNA3.1 sterile vector DNA mixed with 5ul OPTI-DMEM (GIBCO) and 5uL of Lipofectamin 2000 (Invitrogen), and incubated for 5 hours. The media was then replaced with 20% FBS in OPTIDMEM (GIBCO) overnight, and then replaced with 10% FBS in DMEM. Lastly, stable transfection selection was accomplished by administering 25ug/ml

Hygromycin with frequent changes of the drug containing growth media. Hygromycin resistant clones were then isolated and cultured individually, initially in wells of 96 well plates and then transferred onto 24 well plates, expanded in T-25 flasks and maintained in T-75 flasks in 10% FBS DMEM and 10ug/ul Hygromycin. The clones were frozen quickly in growth media containing 50% FBS and 10% dimethyl sulfoxide (DMSO) and their stocks were maintained in liquid nitrogen. (ii) *Luciferase*: Stable expression of Luciferase was achieved by infection with the respective Lentivirus (Lenti-Fire, In Vivo Imaging Solutions, Cheyenne WY 82001) in a 24 well plate at 70% confluency according to the manufactures protocol. The mixture of complete medium and Polybrene (Polybrene®-Hexadimethrine Bromide; Sigma Cat. No. H9268) was made to a final concentration of 5ug/ml and plated at a volume of 0.5ml onto cells. 5ul of Lentivirus stock was added to cells and media/Polybrene mixtures. Cells were incubated at 37C with 5%CO<sub>2</sub> overnight. The following day transfection media was replaced with 1ml of complete pre-warmed medium and incubated at 37C with 5% CO<sub>2</sub> overnight. The cells were selected in puromycin and successful transfections were screened using Luciferase Assay System (Promega, #E1501) using a standard luminometer (Victor 3, Perkin Elmer).

***Tissue Factor Procoagulant Activity Assay (TF PCA):*** Tissue factor procoagulant activities (TF PCAs) of cells lines was measured by means of TF procoagulant assay, as described elsewhere (27, 50). Cells were grown on a 24 well plate (in quadruplicates). When the cells were 70% confluent, they were washed three times with TBS (pH 7.4). Rabbit Brain Thrombin (RBT) (DadeBehring) was prepared in a series of dilutions as control for thrombin (IIa) generation. Cells were then treated with 5nM FVIIa, 150nM FX and 100mM CaCl<sub>2</sub> in TBS and incubated for 30 minutes at 37°C. Prior, 20uL of 2mM S-2765 (CHROMOGENIX) substrate was added to wells of a 96-well plate. After 30 minutes, 200uL of incubated solution was added to the chromogenic substrate and incubated for 3 minutes at 37°C. To stop the reaction 20uL of 50% Acetic Acid was added to each well (of the 96 well plate) before reading TF PCA. To the cells remaining on the 24 well plate, RIPA lysis buffer was added so that protein content

determined in the Bradford Assay (Bio-Rad Bradford Reagent) could be used to normalize the TF PCA readings. The colorimetric reaction in the 96 well plate was read at 405nm on a Lab Systems Multiskan BIOCHROMATIC 1.03 plate reader and TF PCA was then calculated using a nonlinear regression graph (SIGMA PLOT) of the standard RBT samples, and expressed in arbitrary units normalized to the protein content of the corresponding cells. In many of these assays (as indicated) TF-PCA of U373vIII cells was used as a positive control and arbitrarily chosen as 100% value.

***Matrigel Pellets:*** Cold liquid Matrigel (BD Biosciences) was mixed with  $5 \times 10^6$  cells (cell line of interest) and injected subcutaneously in FOX CHASE or YFP SCID mice to form a palpable pellet. Pellets were collected at Day 16 (or as indicated) for a number of experimental endpoints, including flash frozen samples for RNA extraction, samples preserved in 4% PFA for immunohistochemistry and dissociation with dispase for Flow Cytometry.

***Analysis of mRNA Expression:*** For RNA extraction of cells, cells were grown on 10 cm FALCON plates to 70% confluency, washed with DEPC water twice before 1ml of TRIzol Reagent (Invitrogen) was added to each sample then followed by 0.2ml of chloroform. The sample was then vigorously shaken for 15 seconds to shear the DNA and the samples were incubated at 15°C to 30°C for 2 to 3 minutes. Samples were then centrifuged at 12,000 x g for 15 minutes at 2 to 8°C. The aqueous phase was then transferred to a fresh tube and precipitated with 0.5ml isopropyl alcohol at 15 to 30°C for 10 minutes. The precipitate was collected by centrifugation at 12,000xg for 10 minutes (at 2 to 8°C), and the gel-like pellet (RNA) was washed with 75% ethanol (in DEPC-treated water) and then dissolved in RNase free DEPC water, followed by quantification using a (NanoDrop ND-1000, Thermo Scientific) spectrophotometer. For RNA extraction of Day 16 Matrigel pellets were flash frozen immediately after excision from mice and

subjected to RNeasy Plus Mini Kit extraction (Quiagen, #74134) following manufactures recommendations.

**Reverse-Transcriptase PCR (RT PCR):** RNA was transcribed into cDNA and then amplified using a OneStep RT-PCR Kit (QIAGEN). Aliquots of 0.5ug of each RNA preparation was used to carry out the reaction, reverse transcriptase reaction occurred at 50°C for 30minutes in an Eppendorf Mastercycler gradient PCR machine. Once cDNA was generated the following primers were used to amplify the specific gene products.

<b>Gene</b>	<b>Forward Primer</b>	<b>Reverse Primer</b>
hTF	GCTGACTTCAATCCATG	GAAGGTGCCCAGAATACCAA
hGAPDH	GAGTCAACGGATTTGGTCGT	TTGATTTTGGAGGGATCTCG
mTF	TGCTTCTCGACCACAGACAC	TAAAAACTTTGGGGCGTTTG
mPAR1	CTCCTCAAGGAGCAGACCAC	AGACCGTGGAAACGATCAAC
mPAR2	TCTCTGCACCAATCACAAGC	CTTAGCCTTCTTGCCAGGTG
mFVII	TCCAGGGACCTCTAGGGACT	CCTCCGTTCTGACATGGATT
mGAPDH	AACTTTGGCATTGTGGAAGG	ACACATTGGGGGTAGGAACA
RAP1A	CAGGGCCAGAATTTAGCAAG	TTTAGTGCTTGATAGGGAGGAT
TMEM100	GCCTTGTGCTGGAAAGTGAG	TGCCACGAGAGCTGTTTG
SOX11	GGCGAATTCATGGCTTGCAG	GAGATCTCGGCGTTGTGCAT

MYCN	TCCGGAGAGGACACCCTG	GCCTTGGTGTGGAGGAGG
TMEM47	TGGGAGTCCTGCCGCAAACC	TGCCAATCGCTGCTGAGCGT
BCHE	CCAATTTACAGGCTGGAGCAGCA	CCCGATTCTCTGCAACAAAGATGGC
CTSZ	GCACCAGCGCTATGGCGGAT	CCCACCCAGCCACGGAAACG
ID4	CGC TCA CTG CGC TCA ACA C	CTA ACT TCT GCT CTT CCC CC
ID4	GGCCGCGATCGGGCTTAGTC	TGACGGGAGGGTCGCTCTGG
NTRK3	AATGCTCCACATTGCCAGTC	TGAAGATCTCCCAGAGGAT
GRIA1	GGTACGACAAGGGCGAGTGCG	TTCTCTCCACTGCCGCCGCT
UGT8	GACTGGCCGGATCCCAACGC	CTCGCCTCTGACTGCGAGCG
MGP	AACTGGCATCGTGCCCAGGAA	TGGGGGCGGGAAAAAGGGGT
CHRD1	GCGCACTCTAGCTCTCGCCA	AGGAGTCTTCTGGGCAGCGAG
AGXT2L1	GGGATAACGGGAGGAAGGCCG	CTGCCGAGCCAGGCGTAAGG
DDX3Y	CTGGTCACACGTGCTGCGGAA	GCGCCCTTTGCTCGCTGTACT
RPS4Y1	TGCAGCGCCGAAGCATTGGA	CGAATGCCCTTTCCCCTGGGC
SCN3A	GGACCTGGGCAATGTCTCAGCG	AATCGCTTGGGGGCCACTGC
PCDH10	GCCATGATCGTGCTGGCCGT	GCCGGGCTAGAGGAGGCTTT
USP9Y	CTGGCCCTGGCTGTCGTTCC	GGGCTCAGAGGTGAAACTGACCC
KDM5D	GACGAGTTCCTGCCGCCACC	GGCAACTCGAGCCCACCGAC

CIQTNF5	TGAACGAGCAGGGACATTAC	GAAAGAGGCAATGGATTTCGC
ADCYAP1R1	AGACCAAGTCTGGGAGACCGAAAC	ACCGGGCCAGTCGCAAGTAGA
HBE	CCACCCCTGAGGGACACAGGTC	GGGCAATGGCGACAGCAGACA
SPATA22	GACGACGGTTGACGGAGGTCTA	ACAACGGAACAGGCAAACAGCCT
KCNJ16	GCCCAGCTGAAAGCACCTAGCTC	GGGCTCACCAGACGGGCAAG
PYGM	CTAGCGGCCTCCCGCCAATG	CCCCGGAGATCTTCTTGGGGTCC
IF16	GTGGGGTGGAGGCAGGTAAGAAAA	ACCAGCTCATCAGCGAGGCAG
IFITM1	GGACACCACAGCGGCCCTTC	TGGTAGACTGTCACAGAGCCGAA
IFI27	TCTGCCGTAGTTTTGCC	ATCATCTTGGCTGCTATGGAG
KLHL4	ATG TCC AAA AGA CGT GGA GGT	AAC AGC ATC TCG AGG AAC AC
FXVD6	TCTTGGGGACTGGGCTGAGGAC	TCTCGGGCAACAAGCAGCCT
ASTN1	AAGACCCCATGCCCCGTGGT	ATCTCGCTGTAGCGGCACCC
PCDHB6	GCGGACAACGGCCACCTGTT	CTGAACGGGAAGCTATTCCGAGAGG
ALDOC	TGTGGCTGCGGCTGCTAACTG	TGATGCCACACGACGATGCC
NME5	AGGACGGCCGCTGAGCCATAA	CATTGCTCAGGGCTGAGGCGTA
EIFIAY	CGAGGCACAAAGGATGAAAAGG	GGTTCTACAGTTGGGATTTTGGC
RGMA	GTGGCAAGGTTAGGCCCGCA	TCTTGCACGGGGAGGTGGCT



***Tumor Analysis in vivo:*** (i) *Subcutaneous inoculation:* Immunodeficient SCID mice (Charles River), SCID mice harbouring the YFP transgene (YFP/SCID)(55) were injected subcutaneously (s.c.) into the flank region with various glioma cell lines, as indicated. The cells were prepared as a single cell suspension in serum free PBS, tested for trypan blue exclusion to be at least 90% viable, and injected at  $5 \times 10^6$  per mouse in 0.2 ml volume. Alternatively, the same number of 5 millions cells was mixed with cold solution of Matrigel (BD Biosciences) and injected s.c. to form a palpable pellet. The pellets were then removed to analyze tumor cells histologically, as described. Mice injected with tumor cells were monitored several times a week and the emerging tumors were palpated and measured with a digital vernier's caliper. Tumor volume (TV) was calculated, according to the formula:  $TV = (a^2 \times b) \times 0.52$ , where a and b are, respectively, the smaller and the larger perpendicular diameter of the tumor nodule. (ii) *Intracranial inoculation:* YFP transgenic mice were injected intracranially with (50,000 cells/uL with total volume of 2ul) using a Stoelting Stereotaxic Injector at the coordinates (2.5:-1.5:-3.0) of bregma and sagittal suture. All procedures involving animals were performed in accordance with the guidelines of the Canadian Council of Animal Care (CCAC) and the Animal Utilization Protocols (AUP) approved by the Institutional Animal Care Committee (ACC) at MUHC RI and McGill University. When possible, luminescence data was obtained using IVIS 200 scanner. This was done by administering D-Luciferin Firefly potassium salt (Caliper Life Science; 15ug/ml) to mice that had been injected with Luciferase expressing cells followed by imaging.

***Histology, Immunohistochemistry and Immunofluorescence:*** All Matrigel pellets and tumors were preserved in 4% PFA immediately after resection from the mice, upon sacrifice. They were then run through a series of automated processing steps executed in a Leica TP 1050 tissue processor. The resulting paraffin embedded blocks were sectioned using American Optical microtome into 4um thick tissue sections which were placed on pre-coated microscope slides and stored until used. Tumor tissue containing slides were de-waxed in Xylene, and then re-hydrated in a series of alcohol washes (95%

ethanol ->50%ethanol). For tissue visualization by hematoxylin and eosin (H&E) staining rehydrated slides were washed and then incubated with Hematoxylin, 1.5% Acid Solution, pH 2.5, washed in water and then put in Blueing Solution. Slides were then partially dehydrated (50% to 80% ethanol) before being dipped in Eosin solution followed by three five-minute washes in 99% ethanol and Xylene. For immunostaining antigen retrieval was first carried out using Vector Antigen Unmasking Solution heated to 95°C for 15 minutes. Primary antibodies used for these studies were specific for human TF, Endoglin/CD105, and mouse CD45 (Affinity Biological Incorporated #SATF-IG Sheep Anti Human; Goat Anti-Mouse CD105; Cell Signaling #9101 Rat-Anti-Mouse CD45, respectively). Rat anti-mouse F4/80 antibody was purchased from from Abcam (CI:A3-1) ab6640.

These reagents were used at 1:200 dilution overnight in a humidified chamber, at 4°C, and this was followed by three 5min washes in PBS. Fluorescent secondary antibodies (Invitrogen Mouse Anti-sheep Alexa Flour 488, Invitrogen Chicken Anti-Goat Alexa Flour 488, Invitrogen Donkey Anti-Rat Alexa Flour 594, respectively) were incubated with tumor sections in the dark at 37°C for 1hour. After a series of washes with PBS slides were cover slipped using Vectashield Hardset DAPI (Vector) glue. Images were taken on a Zeiss microscope.

**Heatmap:** Heatmaps were generated using MeV software: MeV is part of the [TM4 Microarray Software Suite](#).

**Affymetrix 6.0 SNP Array:** Data were analyzed by Genome Quebec Bioinformatics Department using several programs: APT (Affymetrix Power Tools), PennCNV, Bedtools & R (software for statistical computing and graphics).

**Affymetrix Human Genome U113 2.0 Array:** Data were analyzed through the use of IPA (Ingenuity®systems, [www.ingenuity.com](http://www.ingenuity.com)).

**RRBS Methylation:** RRBS libraries were constructed according to a previously published protocol (1). Briefly, 500ng of DNA from each sample was used in the RRBS experiments and the 10 samples were multiplexed. Samples were then used in paired end sequencing in 1 lane of a HiSeq sequencer (Illumina). BSMAP version 2.6 was used to trim reads (phred quality>30 and Illumina adapters), align reads to hg19 and obtain CpG methylation calls (2). Differentially methylated sequences (individual CpGs and 100 bp tiles) were obtained using Methylkit version 0.5.3 (3). Differentially methylated sequences were annotated using HOMER version 3.51 (4).

**Statistical Analysis:** Data Analysis—All experiments were reproduced at least twice or independently validated with similar results, and numerical data were presented as a number of replicates (n) and mean value of replicates S.D. Statistical analyses were performed using JMP 10.0 (SAS Institute Inc) differences were considered statistically significant when  $p < 0.05$ . A Wilcoxon & Log-rank testing were performed for all mouse experiments. Otherwise, for all other experiments statistical analysis was performed using one-tailed, unpaired t-test.

## **SUPPLEMENTAL DISCUSSION:**

In this study we used the isogenic series of U373 glioma cell lines to explore the link between procoagulant conversion of cancer cells, and their tumor forming capacity. This analysis reinforces the notion that a nexus exists between coagulant properties of cancer cells and their intrinsic genetic and epigenetic make-up. In this particular study, the coagulant phenotype was found to drive the exit of indolent glioma cells from dormancy, in association with early induction of inflammatory and angiogenic hallmarks.

Thus, transformation of parental U373 cells by expression of the EGFRvIII receptor, the most common dominant oncogene in primary glioblastoma (GBM), leads to the onset of aggressive phenotype and dramatic upregulation of tissue factor (TF), as we reported earlier (5). In GBM the *EGFRvIII* mutation coincides with the amplification of the wild type *EGFR* gene, and with overexpression of this growth-driving receptor at the mRNA and protein level. Interestingly, our recent observations suggest that in the classical GBM, characterized by overexpression of EGFR, this property coincides with high endogenous TF level and this is not the case in low-EGFR expressing tumors, such as proneural or neural GBM, but instead these tumors harboured other alterations in their coagulome (6).

It should be mentioned that while upregulation of TF by oncogenic mutations is relatively common (7) this finding may not be entirely universal among cancer cell lines, or absolutely required for their aggressive behavior *in vivo*. However, TF expression may provide a fitness advantage to cancer cells as there is mounting evidence for the contribution of this receptor to angiogenesis, overt tumorigenesis and metastasis (8, 9). What has largely remained unstudied, in this context, is whether these effects of TF include control of very early stages of cancer progression, such as tumor initiation, stemness and cancer

cell dormancy. To our knowledge ours is the first analysis of a link between TF effects and tumor dormancy in the literature, especially as it relates to glioma.

It remains unclear whether and how chronic activation of the coagulation pathway intersects with other mechanisms implicated in tumor dormancy. It is possible that coagulant mechanism may synergize with, and contribute to, regulation of angiogenesis, immune responses and intrinsic growth control processes, as discussed in the recent literature on modulators of the dormant state (10-14). However, it is also possible that these could be alternative biological pathways, or that some mechanisms may be more rate limiting than others. For example, TF-induced inflammatory infiltration could circumvent deficiency in expression of angiogenic factors by cancer cells, as inflammatory cells possess their own angiogenic capacity (15, 16).

The quantitative link between the levels of TF expression (and activity) and the modulation of tumorigenic or dormant cancer cell behaviour remains poorly understood. There is some experimental variability between (and within) different model systems, as to the levels of TF expressed by cancer cells and their corresponding tumorigenic potential. Perhaps the most extreme case is the ability of embryonic stem cells and fibrosarcoma cells to form primary tumors in mice in spite of genetic disruption of their ability to express TF (17-19). We believe that this is to be expected, as different pathways and signalling cues (oncogenes, growth factors, microenvironment) may intersect with the effects of the coagulation system signalling and compensate for deficiency or absence of specific effectors, including TF. We have demonstrated earlier that similar processes and redundant gene expression profiles could also circumvent the effects of some of the central effectors of angiogenesis, such as VEGF (20). While these loss-of-function experiments are informative, the known gain of function effects of VEGF (21) and TF (present

study) can be highly consequential during cancer progression, especially at the early stages of disease development when stromal niche effects are potentially of particular importance.

In this context our choice of the U373 cells as a model and paradigm of dormancy is, at least in part, motivated by their remarkable phenotypic stability and thereby the ability to interrogate aforementioned biological questions. Thus, parental U373 cells express minimal (virtually no) measurable TF, in spite of numerous passages in culture, while maintaining their non-tumorigenic and dormant phenotype *in vivo*. Thus far we observed only one spontaneous tumor arising from such control cells, in spite of numerous injections and extensive manipulation *in vitro* (SI Appendix, Table S1).

Cells isolated from this singular tumor were established in culture, as the S-PT-EV-U373 cell line, and found to manifest markedly elevated expression of TF. Interestingly, similar procoagulant conversion can be observed in several cases of other indolent cancer cell lines subjected to *in vivo* passage, as indicated in Table S1. For example, as we documented earlier Hkh-2 colorectal cancer cells lacking mutant *K-ras* oncogene, and expressing low levels of TF, acquire both of these features following injection and protracted latency in mice (22).

In global terms, tumorigenic conversion of U373 cells can be recapitulated (induced) by the enforced expression of TF at levels comparable to those triggered endogenously by oncogenic EGFRvIII (Table S1). Interestingly, this effect is not observed in clones that ‘failed’ to express appreciable TF levels, but did express some, within the same transfection experiment (Table S1). This suggests that there may not be a linear relationship between TF levels and degree of tumorigenicity, but instead TF must perhaps reach certain functional threshold.

It is of interest to ask, then, how much TF is required for the onset of tumor growth? This, may be difficult to define within the present study (or in general) for several reasons. First, the link between exogenous TF expression and tumorigenic phenotype, as mentioned earlier, seems to be non-linear in nature. For example, tumor takes raise dramatically in our model from ~0 (in control cells) to 60-100%, as a function of high TF expression. However, this change is neither immediate, nor is it complete (100%) in all TF-expressing cell lines (Table S1), of which some exhibit a somewhat lower tumor take in spite of comparable TF levels. This is evident from the comparison of several independent clones, of which TF-U373-D11, -G11, G2 and -B2 exhibit median channel fluorescence for TF surface expression by FACS of approximately 206, 252, 83 and 277 respectively (a change within 330% range). However, the same clones differ in terms of tumor take by only by 10-15% (between 85% and 100% take; SI Appendix, Table S1).

Moreover, the levels of TF expression are modulated *in vivo*. Even clonal cell lines expressing TF homogenously in cell culture reveal a degree of heterogeneity with respect to TF immunofluorescence, when injected into mice (SI Appendix, Fig. S13). This would naturally confound the quantitative link between TF level and tumor promoting activity and may, perhaps reveal unappreciated complexities of this fascinating nexus. We have described this heterogeneity of TF expression *in vivo* in our earlier study, and in this case the modulating influence was linked to changes in cellular differentiation (23).

Finally, our study argues that it is not the TF expression *per se* that drives growth of tumors and their escape from dormancy. Rather, this transition is linked to secondary genetic and epigenetic alterations that are facilitated within the procoagulant microenvironment induced by chronic exposure of TF by cancer cells.

The analysis of tumor dormancy in the literature is often predicated on quantitative comparisons between early and late onsets of tumor growth in specific experimental systems. However, it is possible that more permanent dormant states may exist, in which transformed cells may silently persist in disease-free patients, as documented by Black and Welch, as well as others (24). In this regard, U373 cells are especially informative, as they are transformed and immortal, lack PTEN expression, divide indefinitely in culture and are derived from authentic human glioma, but yet are capable of indefinite dormancy *in vivo*. This is evident from our measurements of Luciferase signal over hundreds of days during, which these cells remain dormant in mice. Dormancy in this particular experimental system is virtually indefinite (during the lifetime of recipient mice), and escape is defined as formation of tumors at any point post cell inoculation.

TF transfection leads to a qualitative change in behavior of U373 cells *in vivo*, without marked changes in their properties *in vitro*. Upon inoculation of TF-expressing U373 cells tumors emerge in the vast majority of, albeit not all, mice and within 60-210 days (Table S1). This is far longer than in the case of U373vIII cells harbouring EGFRvIII oncogene, where growth begins almost immediately after inoculation and leads to a clinical endpoint beginning to emerge within 30 days. We would like to refer to the difference between this latter threshold and the onset of tumors in the case of TF transfectants as “latency” (Fig. 2A), which is meant to signify the difference between the subclinical but implicitly progressive disease (TF-U373 cells), and a true long term dormancy (U373 and EV-U373 control cells).

Events leading to the TF-driven escape from dormancy are set in motion relatively early on (at the microscopic level), and we empirically chose day 16 to examine them in detail. Again, we observed



inflammatory and angiogenic infiltration weeks or months prior to formation of detectable tumors, an observation highlighting the duration of underlying biological changes.

Such inflammatory and angiogenic consequences of the activated coagulation pathway and TF signalling have been explored in the literature by others (25-27) and also by some of our earlier work (5, 22). What these studies did not address, however, is the role of coagulation pathway at very early stages of cancer progression, including the escape from the dormant state, the central question explored in our present report. Our observations suggest that TF-mediated effects lead to early recruitment of endothelial (CD105), hematopoietic (CD45), myeloid (CD11b) and macrophage-like (F4/80) cells into the vicinity of cancer cells. We propose that interactions between host and cancer cells may lead to genetic, epigenetic and phenotypic alterations impacting the natural history of the resulting lesions.

Exit from dormancy represents an operational manifestation of the existence of cells capable of triggering tumor growth. Such cells are often referred to as tumor initiating cells (TICs), or cancer stem cells (CSCs). We do not know whether our PT-series of tumorigenic variants of U373 glioma cells possess overt phenotypic properties of TICs, or glioma stem cells (GSCs), and the related work is currently ongoing. However, these cells do trigger tumor growth and arise in a context of procoagulant and inflammatory niches containing host cell populations. As we argued earlier (28), TICs may receive cues from the coagulation system and from their vascular microenvironment, of which activated endothelial cells are an important part. It is of note that such activated endothelial cells may also express TF (29), and the role of this phenotype is of considerable interest.

In this regard Ghajar et al (30) have recently described dormant behaviour of breast cancer stem cells in association with quiescent vasculature and mediated by thrombospondin 1 (TSP-1), while sprouting endothelium, TGF beta 1 and periostin were able to modulate this silent behaviour and influence tumor onset. These authors did not analyse TF levels, or the activation of coagulation in this setting, but our earlier study suggests that TSP-1 and -2 could be regulated by TF in cancer cells (22). It could be suggested that the vascular niche for certain types of TICs could also involve endothelial TF expression and signalling.

In this context certain complexities should be carefully considered. For example, it should be borne in mind that the tumor forming ability of totipotential embryonic stem (ES) cells could be blocked in TF-deficient (hypomorphic) mice, but only when these ES cells themselves were TF-deficient. In fact, several TF-expressing cancer cell lines are able to grow in TF-hypomorphic mice (19), or mice treated with anti-mouse-TF antibodies (31), which would be expected to block endothelial TF and TF present on other host cells. Since this is insufficient to obliterate tumorigenesis in the majority of models tested thus far, it could be suggested that, while TF expression by endothelial cells could be a hallmark of aggressive cancer, this feature may not possess universal and rate limiting functional impact on tumor initiation.

One of the most striking observations in our study is the emergence of DNA copy number variations (CNV), and DNA methylation in cells that have acquired tumorigenic properties through exposure to the procoagulant microenvironment *in vivo*. Such genetic and epigenetic changes are considered permanent, since they are inheritable across cellular generations and may contribute to cancer in many important ways. This includes expression of transforming oncogenes and silencing of tumor suppressors (32). To our knowledge our report is the first to points out to the possibility of mutational changes resulting from

the chronic activation of the coagulation pathway. We believe that it is the inflammatory infiltration that may play an especially important inductive and selective role in this context.

We also believe that genetic and epigenetic changes associated with the exposure of glioma cells to the coagulant (TF-driven) microenvironment *in vivo*, and escape from dormancy likely occur after and not prior to cell inoculation. This is for several reasons. First, each TF-transfectant we used in our study is a single clone with relatively stable properties, and with characteristics inconsistent with high rate of genetic or epigenetic instability. Hence, time is a key factor in the emergence of tumorigenic variants. In this regard a relatively short culture before injection of TF-U373 cell lines was out of proportion to the lengthy incubation of these cells in Matrigel pellets *in vivo*. Second, Matrigel pellets containing TF-expressing clones contain inflammatory infiltrates that may have mutagenic and selective potential, and such pressures do not exist in culture. Third, if CNV and epigenetic changes were to occur prior to injection, they would have been equally likely in control (EV-U373) and TF-expressing (TF-U373) clones, and this is not what we observed.

Our present report complements the body of work that points to the role of oncogenic events in triggering the expression of TF, coagulant and stromal responses in cancer (22). We presently propose that reverse may also be true, in that the exposure of cancer cells to the chronic activation of the coagulation system, and to the related inflammatory effects, may provoke genetic and epigenetic drift of these cells resulting in escape from dormancy. We think that this is, in a certain way a “chicken and egg” problem, as cancers often develop through perpetual interactions with perturbed microenvironment, which they influence to genetically progress further. This proposed vicious circles is depicted in SI Appendix, Fig. S14.

It is possible that these iterative events are particularly relevant in cancers associated with chronic inflammation. Notably, experimental induction of such tumors in the intestine is dependent on the functionality of the coagulation system (27). Interestingly, in human tumors that arise in a similar manner, as a result of the inflammatory bowel disease, the associated oncogenic mutations include p53, *K-ras* (33), which are known for regulation of TF (22), and angiogenesis (34). Indeed, mutant *K-ras* provokes angiogenesis (34) and triggers inflammatory phenotype in cancer cells (35), in part through upregulation of the respective paracrine mediators (VEGF, IL-8 and others). Analogous processes in the brain have not been studied.

We speculate that the higher propensity to develop colorectal cancer recently reported in patients harboring homozygous Factor V Leiden mutation and associated hypercoagulability (36) may have relevance to dormancy. Thus, as in our study, one could envisage that Factor V Leiden driven thrombophilia, and/or its biological consequences could awaken dormant tumor cells. However, these sorts of comparisons must be entertained very cautiously as other forms of thrombophilia, including heterozygous Factor V Leiden mutation, do not carry the same risk of cancer as FV Leiden homozygosity (36). We would like to argue that it may be the mechanism and magnitude of thrombophilia that could play a role in this diversity, rather the general presence or absence of clinically detected hypercoagulability. Our recent study on molecular subtypes of GBM (6) suggest that different disease mechanisms may provoke diverse patterns of deregulated coagulation factors. These questions require further scrutiny.

We also suggest that the previously proposed connection between head trauma and GBM (37) should, perhaps, be revisited in the context of tumor dormancy. While these findings require careful scrutiny it is intriguing to note that GBM may emerge within the glial scar, or be linked with other aspects of head

trauma, as indicated by several studies (38-42). It is tempting to speculate that such a linkage could involve dormant cells and their interactions with mediators of healing responses elicited by head trauma, including coagulation, inflammation and angiogenesis.

We documented that endothelial (CD105), hematopoietic (CD45), myeloid cells (CD11b), and activated macrophage-like (F4/80) cells are recruited to the sites occupied by of TF-expressing glioma cells, but not (less so) to their dormant counterparts. We suggest that these host cells may play a role in awakening of dormant glioma cells that may respond to paracrine and mutagenic effects of the myeloid and vascular niche. This is consistent with the recently documented role of macrophages in glioma progression (43), and it would be of interest to assess the profiles of soluble and exosomal mediators that may participate in these interactions.

Thus, we interpret our findings as an indication that the coagulation system effectors may contribute to regulation of the quiescent behavior of tumor (initiating) cells or their escape from dormancy, either by activation of the clotting machinery itself, or by signalling events, or both. This is likely executed with the contribution of the recruited host cells and through mechanisms that impact cancer cell genome, epigenome phenotype and growth. We believe that these possibilities are meaningful, and we see our study as voice in discussion on the role of coagulation in biology of brain tumors and potential applications of anticoagulants in this context.

## **SUPPLEMENTARY FIGURE LEGENDS:**

**Figure S1. Generation and characterization of S-PT and B-PT series of tumorigenic glioma cell lines.** **A.** Expression of TF and generation of tumorigenic variants does not impact in vitro growth kinetics of U373-derived glioma cells. MTS assay were performed at normoxia shows no proliferative differences of TF-clones, S-PT series of cells and parental U373 cells. **B.** Similarly, under hypoxic conditions all cells lines, with exception of U373vIII, grew at similar proliferative rates. **C.** S-PT cell lines express high TF levels as revealed by FACS. **D.** Diagrammatic representation of subcutaneous primary tumor (S-PT) and brain primary tumor (B-PT) cell line generation. TF-U373 transfected cell lines were used to generate tumors which were excised and cultured. **E.** In vivo fates of U373 derived cell lines and their abilities to generate tumors in mice. Only 1 injection of parental (TF non-expressing) U373 cells eventually led to tumor formation. Cells derived from this tumor were highly TF positive. **F.** Similar morphology of U373 and TF-U373 cells (clones G11 and D11) in vitro. These cells differ from more spindly cells of the corresponding tumor-derived (PT)series: S-PT-TF-U373 (G11 and D11).

**Figure S2. Changes gene expression in tumor cells in vivo as a function of tissue factor-related changes in microenvironment.** **A.** Survey of changes in human gene expression profiles between glioma cells contained in Matrigel pellets in vivo. Heatmap of Affymetrix Human Genome Array U133 plus 2.0 analysis performed on mRNA preparations from pellets containing EV U373 or TF U373 G11 cells on day 16 days post inoculation. Top 10 up-regulated and 10 down-regulated genes. **B** List of differentially expressed genes that were validated by semi-quantitative RT-PCR. **C.** Table of top 3 Networks identified in response to TF expression, using IPA software, including genes with at least 2 fold change in expression (up or down).

**Figure S3: Enforced expression of human TF in U373 leads to formation of palpable tumors.** **A.** RT-PCR of cell lines confirms successful transfection and incorporation of full length human TF onto parental non-TF expressing U373 cells. **B.** Escape from dormancy by TF expressing cells (TF-U373-G11) as indicated by obvious tumors on day 110 post injection.

**Figure S4. Patterns of glioma cell growth in vivo.** **A.** S-PT series of cell lines grow rapidly in vivo compared to their TF-clone counterparts.

**Figure S5: Network 1: Cellular Movement, Genetic Disorder, Neurological Disease.** **A.** IPA software indicates this network to be the most relevant with a score of 87 in the comparison between Day 16 gene expression profiles of EV-U373 and TF-U373-G11 cells (2 fold change or greater was considered).

**Figure S6: Network 2: Cell Movement, Cancer, Immune Cell Trafficking.** **A.** IPA software indicates this network to be the second most relevant with a score of 56 in the comparison between Day 16 gene expression profiles of EV-U373 and TF-U373-G11 cells (2 fold change or greater was considered)

**Figure S7: Network 3: Cancer, Cellular Growth and Proliferation, Cellular Development.** **A.** IPA software indicates this network to be the third most relevant with a score of 53 in the comparison between Day 16 gene expression profiles of EV-U373 and TF-U373-G11 cells (2 fold change or greater was considered).

**Figure S8: Network 1: Cancer, Gene Expression, Cell Cycle.** A. IPA software indicates this network to be the most relevant with a score of 134 in the comparison between Day 16 gene expression profiles of TF-U373-G11 and S-PT-U373-G11 cells (2 fold change or greater was considered)

**Figure 9 Network 2: Inflammatory Response, Cellular Movement, Cancer.** IPA software indicates this network to be the second most relevant with a score of 61 in the comparison between Day 16 gene expression profiles of TF-U373-G11 and S-PT-U373-G11 cells (2 fold change or greater was considered)

**Figure S10: Network 3: Cell Cycle, Cell Death, Cellular Growth and Proliferation.** IPA software indicates this network to be the third most relevant with a score of 42 in the comparison between Day 16 gene expression profiles of TF-U373-G11 and S-PT-U373-G11 cells (2 fold change or greater was considered)

**Table S1: Dormancy, latency and growth of TF expressing and non expressing cancer cell of different origin.** Transition from indolent or latent to tumorigenic phenotype is associated with increase in TF expression.

**Figure S11: SNP analysis of TF-expressing and tumorigenic variants derived from the U373 glioma cell line.** Enlarged version of the image presented in Figure 4A to visualize DNA copy number variation between the cells in individual chromosomes.



**Figure S12: RRBS analysis of DNA methylation pattern in TF-expressing and tumorigenic variants derived from the U373 glioma cell line.** Enlarged version of the image presented in Figure 4B, to visualize details of the heatmap depicting methylation patterns of 8 different cell lines representing 4 pairs of TF-transfected U373 clones (B2, D11, G11,G2) and their corresponding derivatives (PT) obtained after formation of subcutaneous tumors in mice (as described in the text).

**Figure S13: Diversity of TF levels in vivo among glioma cells expressing uniform levels of TF in vitro.** U373vIII cells express uniform and high level of TF in culture (see text). However, while growing as tumors in mice some of the cells remain brightly positive for TF antigen, while the signal for other cells is somewhat diminished. Similar properties were observed in other TF-expressing glioma cells (compare Table S1) and were described in our earlier study (23).

**Figure S14: Reciprocal interrelationship between microenvironment and cancer cell genome – a hypothesis.** TF-driven procoagulant microenvironment triggers inflammatory, angiogenic and other extracellular pressures that induce and select for genetic and epigenetic changes within cancer cells. This genotypic drift affects coagulant, inflammatory and angiogenic aspects of the cellular phenotype and secretome, which may further alter tumor microenvironment leading to adaptive cycles of tumor progression (vicious circle).

## SI APPENDIX - REFERENCES

1. Saeed AI., Sharov V, White J, Li J, Liang, et al (2003) TM4: a free, open-source system for microarray data management and analysis. *Biotechniques*. **34**: 374-378.
2. Boyle P, Clement K, Gu H, Smith ZD, Ziller M, et al (2012) Gel-free multiplexed reduced representation bisulfite sequencing for large-scale DNA methylation profiling. *Genome Biol.* **13**: R92.
3. Xi, Y. & Li, W. (2009) BSMAP: whole genome bisulfite sequence MAPping program. *BMC Bioinformatics* **10**:232. doi: 10.1186/1471-2105-10-232, 232-10.
4. Akalin A, Kormaksson M, Li S, Garrett-Bakelman FE, Figueroa ME, et al. (2012) methylKit: a comprehensive R package for the analysis of genome-wide DNA methylation profiles. *Genome Biol.* **13**:R87.
5. Garnier D, Milsom C, Magnus N, Meehan B, Weitz J, et al (2010) Role of the tissue factor pathway in the biology of tumor initiating cells. *Thromb. Res.* **125** Suppl 2:S44-50.
6. Magnus N, Gerges N, Jabado N, Rak J. (2013) Coagulation-related gene expression profile in glioblastoma is defined by molecular disease subtype. *J. Thromb. Haemost.* **11**:1197-1200.
7. Magnus N, D'Asti E, Garnier D, Meehan B, Rak J (2013) Brain neoplasms and coagulation. *Semin. Thromb. Hemost.* **39**:881-895.
8. Palumbo JS, Talmage KE, Massari JV, La Jeunesse CM, Flick MJ et al (2007) Tumor cell-associated tissue factor and circulating hemostatic factors cooperate to increase metastatic potential through natural killer cell-dependent and-independent mechanisms. *Blood.* **110**:133-141.
9. Versteeg HH, Schaffner F, Kerver M, Petersen HH, Ahamed J et al (2008) Inhibition of tissue factor signaling suppresses tumor growth. *Blood* **111**:190-199.
10. Almog, N. (2010) Molecular mechanisms underlying tumor dormancy. *Cancer Lett.* **294**:139-146.
11. Aguirre-Ghiso JA. (2007) Models, mechanisms and clinical evidence for cancer dormancy. *Nat. Rev. Cancer* **7**:834-846.
12. Naumov GN, Folkman J, Straume O (2009) Tumor dormancy due to failure of angiogenesis: role of the microenvironment. *Clin Exp. Metastasis.* **26**:51-60.
13. Goss PE, Chambers AF (2010) Does tumor dormancy offer a therapeutic target? *Nat. Rev. Cancer.* **10**:871-877.
14. Uhr JW, Pantel K (2011) Controversies in clinical cancer dormancy. *Proc. Natl. Acad. Sci. U. S. A.* **108**:12396-12400.

15. Mantovani A, Allavena P, Sica A, Balkwill F (2008) Cancer-related inflammation. *Nature* 454:436-444.
16. Phan VT, Wu X, Cheng JH, Sheng RX, Chung AS et al (2013) Oncogenic RAS pathway activation promotes resistance to anti-VEGF therapy through G-CSF-induced neutrophil recruitment. *Proc. Natl. Acad. Sci. U. S. A.* 110:6079-6084.
17. Toomey JR, Kratzer KE, Lasky NM, Broze GJ Jr. (1997) Effect of tissue factor deficiency on mouse and tumor development. *Proc. Natl. Acad. Sci. U. S. A.* 94:6922-6926.
18. Palumbo JS, Degen JL (2007) Mechanisms linking tumor cell-associated procoagulant function to tumor metastasis. *Thromb. Res.* 120 Suppl 2:S22-S28.
19. Yu J, May L, Milsom C, Anderson GM, Weitz JI et al (2008) Contribution of host-derived tissue factor to tumor neovascularization. *Arterioscler. Thromb. Vasc. Biol* 28:1975-1981.
20. Vilorio-Petit A, Miquerol L, Yu JL, Gertsenstein M, Sheehan C et al (2003) Contrasting effects of VEGF gene disruption in embryonic stem cell-derived versus oncogene-induced tumors. *EMBO J* 22:4091-4102.
21. Kim I, Oh JL, Ryu YS, So JN, Sessa WC et al (2002) Angiopoietin-1 negatively regulates expression and activity of tissue factor in endothelial cells. *FASEB J* 16:126-128.
22. Yu JL, May L, Lhotak V, Shahrzad S, Shirasawa S et al (2005) Oncogenic events regulate tissue factor expression in colorectal cancer cells: implications for tumor progression and angiogenesis. *Blood* 105:1734-1741.
23. Milsom C, Yu J, May L, Magnus N, Rak J (2008) Diverse roles of tissue factor-expressing cell subsets in tumor progression. *Semin. Thromb. Hemost.* 34:170-181.
24. Black WC, Welch HG (1993) Advances in diagnostic imaging and overestimations of disease prevalence and the benefits of therapy. *New Engl. J. Med.* 328:1237-1243.
25. Abe K, Shoji M, Chen J, Bierhaus A, Danave I et al (1999) Regulation of vascular endothelial growth factor production and angiogenesis by the cytoplasmic tail of tissue factor. *Proc. Natl. Acad. Sci. U. S. A.* 96:8663-8668.
26. Versteeg HH, Schaffner F, Kerver M, Ellies LG, Andrade-Gordon P et al (2008) Protease-activated receptor (PAR) 2, but not PAR1, signaling promotes the development of mammary adenocarcinoma in polyoma middle T mice. *Cancer Res.* 68:7219-7227.
27. Steinbrecher KA, Horowitz NA, Blevins EA, Barney KA, Shaw MA et al (2010) Colitis-associated cancer is dependent on the interplay between the hemostatic and inflammatory systems and supported by integrin alpha(M)beta(2) engagement of fibrinogen. *Cancer Res.* 70:2634-2643.

28. Milsom C, Magnus N, Meehan B, Al-Nedawi K, Garnier D et al (2009) Tissue factor and cancer stem cells: is there a linkage? *Arterioscler. Thromb. Vasc. Biol.* 29:2005-2014
29. Contrino J, Hair G, Kreutzer DL, Rickles FR (1996) In situ detection of tissue factor in vascular endothelial cells: correlation with the malignant phenotype of human breast disease. *Nat. Med.* 2:209-215.
30. Ghajar CM, Peinado H, Mori H, Matei IR, Evason KJ et al (2013) The perivascular niche regulates breast tumor dormancy. *Nat. Cell Biol.* 15:807-817.
31. Ngo CV, Picha K, McCabe F, Millar H, Tawadros R et al (2007) CNTO 859, a humanized anti-tissue factor monoclonal antibody, is a potent inhibitor of breast cancer metastasis and tumor growth in xenograft models. *Int. J. Cancer* 120:1261-1267.
32. You JS, Jones PA (2012) Cancer genetics and epigenetics: two sides of the same coin? *Cancer Cell.* 22:9-20.
33. Leedham SJ, Graham TA, Oukrif D, McDonald SA, Rodriguez-Justo M et al (2009) Clonality, founder mutations, and field cancerization in human ulcerative colitis-associated neoplasia. *Gastroenterology.* 136:542-550.
34. Rak J, Mitsuhashi Y, Bayko L, Filmus J, Sasazuki T et al (1995) Mutant ras oncogenes upregulate VEGF/VPF expression: implications for induction and inhibition of tumor angiogenesis. *Cancer Res.* 55:4575-4580.
35. Sparmann A, Bar-Sagi D (2004) Ras-induced interleukin-8 expression plays a critical role in tumor growth and angiogenesis. *Cancer Cell* 6:447-458.
36. Vossen CY, Hoffmeister M, Chang-Claude JC, Rosendaal FR, Brenner H (2011) Clotting factor gene polymorphisms and colorectal cancer risk. *J Clin Oncol.* 29:1722-1727.
37. Hochberg F, Toniolo P, Cole P (1984) Head trauma and seizures as risk factors of glioblastoma. *Neurology.* 34:1511-1514.
38. Mrowka R, Bogunska C, Kulesza J, Bazowski P, Wencel T (1978) Grave cranio-cerebral trauma 30 years ago as cause of the brain glioma at the locus of the trauma particulars of the case. *Zentralbl. Neurochir.* 39:57-64.
39. Preston-Martin S, Pogoda JM, Schlehofer B, Blettner M, Howe GR et al (1998) An international case-control study of adult glioma and meningioma: the role of head trauma. *Int. J Epidemiol.* 27:579-586.
40. Henry PT, Rajshekhar V (2000) Post-traumatic malignant glioma: case report and review of the literature. *Br. J Neurosurg.* 14:64-67.

41. Magnavita N, Placentino RA, Mei D, Ferraro D, Di TG (2003) Occupational head injury and subsequent glioma. *Neurol. Sci.* 24:31-33.
42. Anselmi E, Vallisa D, Berte R, Vanzo C, Cavanna L (2006) Post-traumatic glioma: report of two cases. *Tumori.* 92:175-177.
43. Pyonteck SM, Akkari L, Schuhmacher AJ, Bowman RL, Sevenich L et al (2013) CSF-1R inhibition alters macrophage polarization and blocks glioma progression. *Nat. Med.* 19:1264-1272.